AIP | Journal of Applied Physics

Intermixing of InGaAs/GaAs quantum wells and quantum dots using sputter-deposited silicon oxynitride capping layers

Ian McKerracher, Lan Fu, Hark Hoe Tan, and Chennupati Jagadish

Citation: J. Appl. Phys. **112**, 113511 (2012); doi: 10.1063/1.4768283
View online: http://dx.doi.org/10.1063/1.4768283
View Table of Contents: http://jap.aip.org/resource/1/JAPIAU/v112/i11
Published by the American Institute of Physics.

Intermixing of InGaAs/GaAs quantum wells and quantum dots using sputter-deposited silicon oxynitride capping layers

Ian McKerracher,[a] Lan Fu, Hark Hoe Tan, and Chennupati Jagadish
Department of Electronic Materials Engineering, Research School of Physics and Engineering, The Australian National University, Canberra, Australian Capital Territory 0200, Australia

(Received 8 August 2012; accepted 6 November 2012; published online 6 December 2012)

Various approaches can be used to selectively control the amount of intermixing in III-V quantum well and quantum dot structures. Impurity-free vacancy disordering is one technique that is favored for its simplicity, however this mechanism is sensitive to many experimental parameters. In this study, a series of silicon oxynitride capping layers have been used in the intermixing of InGaAs/GaAs quantum well and quantum dot structures. These thin films were deposited by sputter deposition in order to minimize the incorporation of hydrogen, which has been reported to influence impurity-free vacancy disordering. The degree of intermixing was probed by photoluminescence spectroscopy and this is discussed with respect to the properties of the SiO_xN_y films. This work was also designed to monitor any additional intermixing that might be attributed to the sputtering process. In addition, the high-temperature stress is known to affect the group-III vacancy concentration, which is central to the intermixing process. This stress was directly measured and the experimental values are compared with an elastic-deformation model. © *2012 American Institute of Physics*. [http://dx.doi.org/10.1063/1.4768283]

I. INTRODUCTION

The optoelectronic properties of quantum well (QW) and quantum dot (QD) structures can be altered after the initial growth by intermixing techniques.[1] These usually involve high-temperature processes whereby atoms from within the QW or QD regions are interdiffused with barrier atoms. Selective-area intermixing enables different components to be monolithically integrated, such as lasers and waveguides.[2] In comparison, traditional etch-and-regrowth methods are time-consuming and the resulting interfaces can increase optical losses.[3]

Selective intermixing may involve enhancing interdiffusion in specific areas of a sample by laser-induced intermixing or impurity-induced disordering (IID).[4–6] Intermixing can also be enhanced through impurity-free vacancy disordering (IFVD), whereby the semiconductor is capped with a dielectric film prior to high-temperature annealing. IFVD may be preferred to other techniques because few impurities are introduced and this results in higher quality material.[6] In addition, it is relatively straight-forward to perform intermixing with dielectric capping layers. The degree of intermixing, however, is sensitive to a plethora of experimental parameters including the film properties, the specific semiconductor materials and the annealing conditions.[1,7–9]

In this study, intermixing is performed on InGaAs/GaAs QW and QD samples. In these III-V materials, interdiffusion occurs between In atoms from the QW or QD, and Ga atoms from the barrier layers. Silica capping layers are usually chosen for IFVD and annealing is typically performed between 600 °C and 1000 °C.[1,7] At these temperatures Ga is highly soluble in the capping layer. When Ga atoms out-diffuse, they leave vacancies (V_{Ga}) in their stead and these promote intermixing in the QWs or QDs below. Ga out-diffusion is promoted by porous silica films, such as those deposited by plasma-enhanced chemical vapor deposition (PECVD) at low temperatures[8] or electron-beam evaporation.[10] Over-stoichiometric SiO_x films (in which $x > 2$) have also been correlated with an increased concentration of V_{Ga} created at the encapsulant-semiconductor interface.[9]

The movement of these vacancies in the III-V matrix during annealing is not only governed by simple diffusion. Due to the large mismatch in the coefficients of thermal expansion (CTE) of silica and GaAs, compressive stress is imposed on the semiconductor at high temperatures. This stress can enhance the mobility of the V_{Ga} and increase the interdiffusion rate in buried heterostructures.[11] On the other hand, compressive stress has also been correlated with the creation of EL2 defects in GaAs. That is, Ga vacancies combine with As interstitials (As_i) to form antisite defects (As_{Ga}).[12] By consuming V_{Ga}, the degree of intermixing may be reduced,[13] so the relationship between stress and the IFVD mechanism is not straight-forward.

Whereas silica is typically used to enhance intermixing, other dielectrics such as TiO_2 or MgF_2 can suppress the amount of thermal interdiffusion.[14–16] With these capping layers, Ga out-diffusion is minimal and the CTE mismatch is reversed. Hence, any vacancies that are created (or indeed present in the as-grown structure) will be trapped at the semiconductor-encapsulant interface and so intermixing is inhibited.[11,17] Silicon nitride (SiN_y) or silicon oxynitride (SiO_xN_y) capping layers have been known to either enhance or suppress intermixing depending on the film characteristics.[18,19] Hydrogen-rich silicon nitride deposited by chemical vapor deposition (CVD) with high NH_3/N_2 ratios is thought to favor Ga out-diffusion and therefore promote IFVD.[19] In the

[a] Electronic mail: ian109@physics.anu.edu.au.

absence of NH_3, PECVD SiO_xN_y films[10] promote more IFVD when $x \gg y$. This suggests that silica can enhance intermixing more effectively than silicon nitride films, however including NH_3 as a precursor for PECVD SiO_xN_y films can complicate the degree of Ga out-diffusion.[20]

The use of TiO_2, fluorides or more exotic thin films for intermixing can bring additional fabrication challenges, such as the development of etching processes. SiO_2, SiN_y and SiO_xN_y films are already widely used in a variety of fields, such as microelectronics and photonics.[21,22] Hence, the ability to reproducibly tune QWs or QDs using the latter set of materials is highly desirable. If the properties of silica films are optimised for IFVD and SiN_y films can suppress intermixing, then specific SiO_xN_y compositions will allow control over the degree of selective intermixing. Systematic studies on the influence of stress, hydrogen content or other film properties are of great value to correlating the amount of intermixing with SiO_xN_y stoichiometry.

Here, silicon oxynitride films have been deposited by magnetron sputter deposition and used as capping layers for intermixing. With only Ar used as the sputtering gas, these films do not contain significant H concentrations. Hence, the high-temperature solubility of Ga should be determined by the SiO_xN_y stoichiometry and the stress will also influence the degree of intermixing. In addition to IFVD, sputter-deposited films have also been shown to enhance intermixing through the creation of surface defects.[23,24] Compared with PECVD, sputtered adatoms are usually deposited with higher energies. If this bombardment creates point defects in the semiconductor surface then intermixing can occur at lower temperatures, to a larger extent and in a range of III-V materials systems.[23]

The aim of this work is to investigate the influence of sputtered SiO_xN_y composition and stress on the degree of intermixing. These experiments were also designed to measure any intermixing induced through the sputtering process. The composition and thermomechanical properties of these films have been reported elsewhere,[25] and these results complement the intermixing study presented here. The extent of intermixing was determined from low-temperature photoluminescence (PL) spectroscopy, which is sensitive to the composition and dimensions of the QWs or QDs. Each PL sample contained a single QW or a single QD layer and no dopants were introduced. Although these are simpler than typical III-V device structures, this ensures that the results are not complicated by IID or other processes. In addition, the high-temperature biaxial stress was measured in these films from similar GaAs samples. This stress is found to be greater than that predicted from the properties of the materials. In fact, this stress is shown to be more significant to the degree of intermixing than the stoichiometry or density of the SiO_xN_y capping layers.

II. EXPERIMENTAL TECHNIQUES

A. Sample preparation

The three III-V structures studied here were grown by metal-organic chemical vapor deposition (MOCVD) on semi-insulating GaAs substrates. In each case, a 200 nm GaAs layer was firstly grown at 720 °C to planarize the surface. This was followed by the thin InGaAs layer and then a further 100 nm of GaAs. Two of these structures contained a single $In_xGa_{1-x}As$ QW grown at 650 °C, which was flanked by the GaAs barriers. The QW was either composed of 15% or 32% In, but was 5 nm thick in both cases. The third structure contained a layer of InGaAs QDs, with a nominal composition of $In_{0.5}Ga_{0.5}As$. This layer was grown at a lower temperature of 550 °C, nominally 5.7 monolayers were deposited and the other QD growth parameters have been described elsewhere.[26]

From each wafer, five PL samples were cleaved that were 3 mm wide and 9 mm long. After degreasing in solvents, each sample was prepared as detailed previously.[27] Essentially, one end of each sample was protected by Al foil while a layer of SiO_xN_y was deposited by sputter deposition. After sputtering, two-thirds of the sample were protected with wax while the film was etched from the other end using HF acid. After again cleaning in solvents, each sample contained three sections: the middle area had been exposed to the sputtering process and was capped with 150–200 nm of SiO_xN_y, one end had been exposed to sputtering but then the capping layer had been removed and the other uncapped end had been protected from the sputtering process. Preparing the two sample ends in this way allowed the effects of physical bombardment during sputter deposition to be studied.

In addition to three PL samples loaded for each SiO_xN_y deposition, a narrow piece of GaAs was also loaded that was used for high-temperature stress measurements. Whereas the substrates previously used[25] to extract the CTE of each SiO_xN_y film had been mechanically polished, the 1 mm wide samples discussed in this article were not thinned. These were clipped directly onto the sample plate and the biaxial stress is expected to be the same as in the PL samples.

The thin films were deposited by magnetron sputter deposition. Five different SiO_xN_y compositions were deposited by simultaneously sputtering SiO_2 and Si_3N_4 targets with different RF powers. More information regarding these depositions has been published previously[25] and it should be noted that the samples discussed in this article were deposited at the same time. Hence, any variations that might arise in subsequent sputtering runs have been avoided. The five films were labelled *A*, *B*, *C*, *D* and *E*, in order of increasing N content and decreasing O content.

To initiate intermixing in the fifteen PL samples, rapid-thermal annealing (RTA) under Ar flow was carried out for 60 s. The ten QW samples were annealed at 850 °C whereas the five QD samples were annealed at only 800 °C, because QD structures are known to have a lower thermal stability.[7] In each case, the samples were placed face-down between two pieces of fresh GaAs to minimise the desorption of As during RTA.

B. Photoluminescence measurements

After annealing, the PL samples were loaded into a portable cryostat, along with an as-grown piece of each structure. After evacuating the Dewar and cooling with liquid nitrogen, low-temperature PL spectra were measured. A 532 nm frequency-doubled solid-state laser was used for excitation,

which was modulated by a chopper rotating at about 330 Hz. The PL emission was focussed into a 50 cm spectrometer that was coupled to a cooled InGaAs photodiode and a lock-in amplifier.

The peak wavelength from each PL spectrum was converted to the photon energy and the energy shift (ΔE) was extracted with respect to the appropriate reference spectrum. That is, the shift attributable to thermal interdiffusion of the QW/QDs (ΔE_{RTA}) was determined by comparing the PL in the Al-protected areas with the as-grown PL. Similarly, the PL shifts associated with sputtering damage (ΔE_{damage}) were extracted by comparing the etched areas with respect to the protected areas of each sample. The shifts due to IFVD (ΔE_{IFVD}) were determined from the oxynitride-capped areas compared to the respective etched areas.

C. High-temperature stress measurements

The biaxial stress in the narrow SiO_xN_y-GaAs samples was determined by measuring their curvature with a Bruker (Veeco) NT9100 optical profiler. Initially, four low-magnification images were stitched together and the curvature was extracted from 3 to 5 mm long regions of the scan, away from the shadow of the sputtering sample clip. The as-deposited stress was determined by comparing the post-deposition radius of curvature (r) with the initial radius of curvature of the uncapped GaAs surface (r_0), which had been measured in the same way.

A Linkam TS1500 microscope stage was then used for measuring the sample curvature at elevated temperatures. A through-transmissive-media module was fitted to the optical profiler and a piece of quartz, similar to the TS1500 cover glass, was placed in the reference arm of the Michelson interferometer. The narrow GaAs samples were cleaved to fit inside the ceramic crucible and they were placed on a sapphire cover slip. The samples were individually loaded, adjacent to a K-type thermocouple that was also positioned in the crucible. The thermocouple was used to calibrate the stage and then for all temperature readings.

During heating, the stage was purged with Ar flowing at about 1 l/min. After again measuring the radius of curvature at room temperature, the sample was heated and r was measured at setpoints of 200 °C, 400 °C and then for every 100 °C up to 900 °C. During cooling, measurements were repeated at the same temperature setpoints. The annealing time for each sample was minimised by using the highest ramp rate of of 130 °C/min, by only waiting a few seconds for each temperature to stabilize and by only collecting a single frame for each curvature measurement. Despite this, measuring each sample took about fifteen minutes and this included five minutes above 600 °C.

III. RESULTS AND ANALYSIS

A. Photoluminescence

The PL measured at 77 K from the three as-grown structures is shown in Fig. 1. The $In_{0.15}Ga_{0.85}As$ QW and the $In_{0.32}Ga_{0.68}As$ QW exhibit PL peaks at 871 nm and 970 nm, respectively. The single-layer QD has the least-intense PL

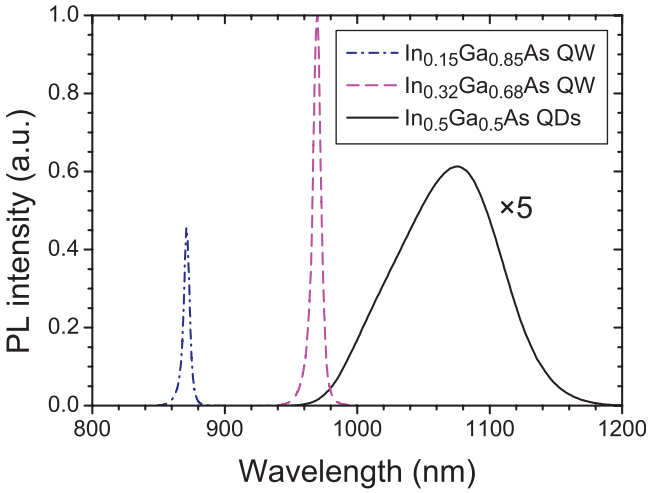

FIG. 1. Photoluminescence spectra at 77 K from the as-grown structures. The QD PL has been fitted with Gaussian peaks to show the dominant QD transitions and the short-wavelength shoulder from the wetting-layer PL.

because inhomogeneities in the QD size and In distribution result in broadening of the peak, which occurs at 1076 nm.

Figure 2 shows the PL spectra from selected annealed samples. One sample from each of the three structures is

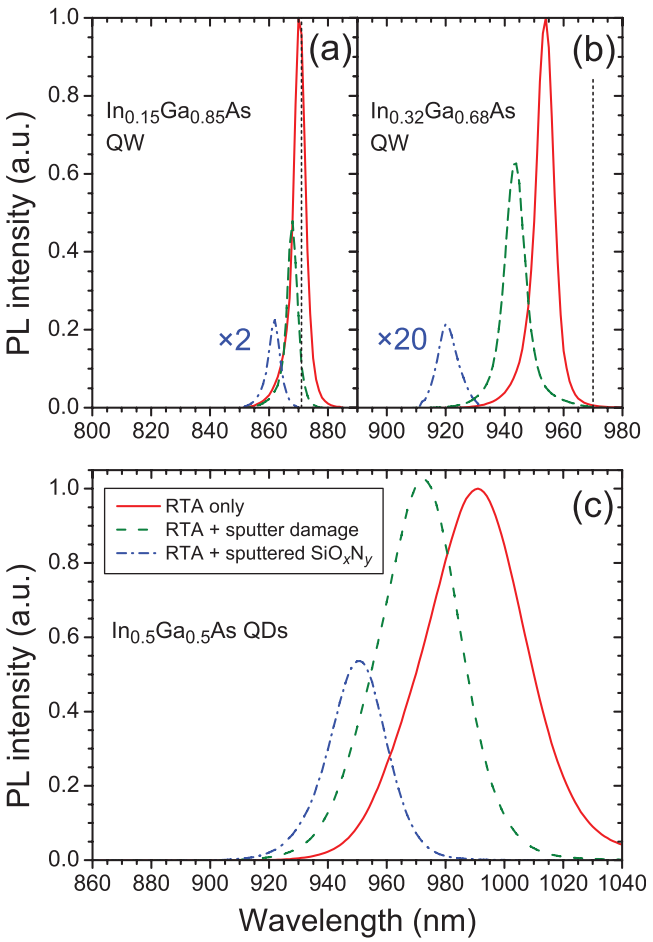

FIG. 2. 77 K PL from (a) the $In_{0.15}Ga_{0.85}As$ QW, (b) the $In_{0.32}Ga_{0.68}As$ QW and (c) the QD samples that were capped with SiO_xN_y film B ($n = 1.50$). The QW samples were annealed at 850 °C and the QDs at 800 °C, each for 60 s. Spectra from all three areas of each sample are shown, indicating the different intermixing contributions. The vertical broken lines in (a) and (b) indicate the wavelengths of the respective as-grown QW peaks.

shown, and the three curves in each set show PL from the three different areas of that sample. These samples were capped with silicon oxynitride film *B*, which was found[25] to have a refractive index of $n = 1.50$ and a composition of $SiO_{2.1}N_{0.1}Ar_{0.02}$. Compared to the as-grown PL in Fig. 1, the red solid lines in Fig. 2 have been blue-shifted by thermal intermixing. The green dashed curves show that the PL from the HF-etched areas is further blue-shifted (ΔE_{damage}) in comparison to the Al-foil protected areas. This suggests that there may have been some surface damage to these samples induced during the sputtering process. The blue broken curves, however, are shifted even further and these additional energy shifts are indicative of IFVD. The latter spectra were measured from the middle third of each sample, which was still capped with silicon oxynitride during RTA. By calculating the energy shifts from the respective green dashed curves (ΔE_{IFVD}), the degree of IFVD was ascertained.

The PL linewidth from each QW has increased after intermixing and this may be a direct result of the smaller confinement potential. Alternatively, the broadened linewidths might be ascribed to inhomogeneities in the intermixing across each QW sample. The PL measurements probe relatively large areas so a superposition of these inhomogeneities is seen. In contrast, the QD linewidth initially decreases with intermixing because of In redistribution during RTA. As a result, the compositional profile in different QDs will be more consistent after annealing and a narrower PL spectrum is observed. This is also accompanied by a slight increase in peak intensity, although the integrated PL area was found to decrease. With extensive intermixing, the QD confinement eventually becomes very shallow and this leads to weaker and broader PL spectra, as seen with the QWs.

The PL from the uncapped area (RTA only) in Fig. 2(a) shows very little shift from the as-grown spectrum, whereas the corresponding peak in Fig. 2(b) exhibits a 21 meV blue-shift. These different degrees of thermal interdiffusion result from the higher concentration gradient in the QW with 32% In. The lattice-mismatch between InGaAs and GaAs also leads to intrinsic strain, however there are differing views as to whether this effect plays a significant role in QW intermixing.[28–30] The red solid curve in Fig. 2(c) shows the QD PL from the uncapped sample area and the peak has been shifted by 84 nm (almost 100 meV) from the as-grown curve in Fig. 1. This suggests an even larger degree of thermal interdiffusion, despite the fact that the QD samples were annealed at only 800 °C. The concentration gradient and intrinsic strain are even higher in the QD structure, however the most significant effect results from the fact that this structure was grown by MOCVD at a lower temperature than the QW structures. A low growth temperature leads to more defects in the III-V material and these will enhance the intermixing process during RTA.[7] The large QD surface area may also play a role in the interdiffusion process.

The additional intermixing contribution caused by the sputtering process was extracted from the HF-etched and protected areas of each sample. These energy shifts are shown in Fig. 3(a) for all fifteen PL samples. The different silicon oxynitride capping layers are represented by their refractive indices at visible wavelengths, which have been shown to

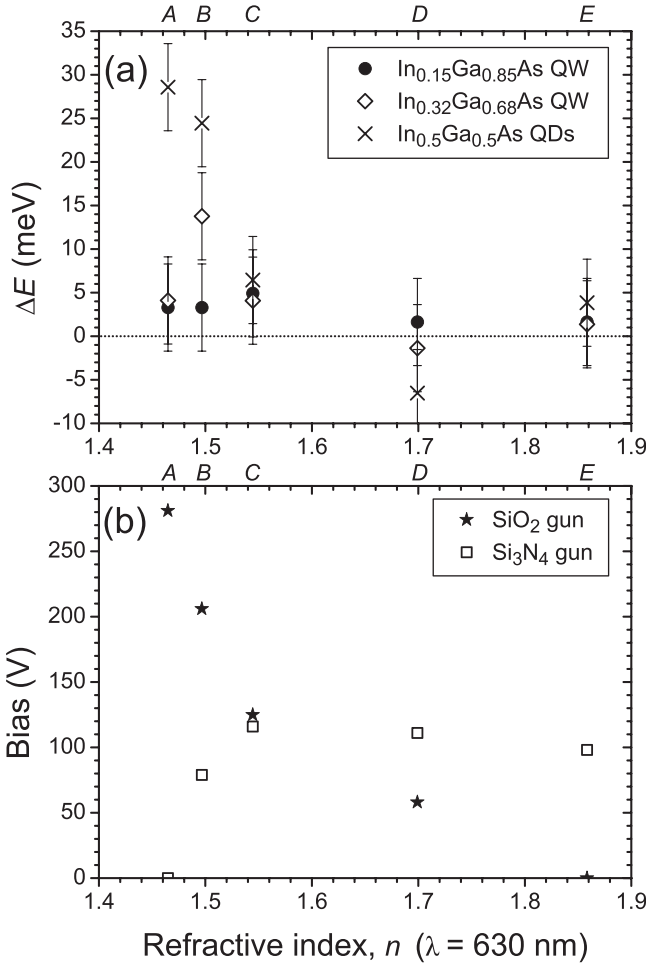

FIG. 3. Surface damage created during sputter deposition may lead to enhanced intermixing. For all five SiO_xN_y films (which are labelled along the top), the 77 K PL shifts in the etched sample areas with respect to the protected areas are shown in (a). The DC bias voltages observed for both guns during sputtering are given in (b).

increase as the films become richer in N and simultaneously deficient in O.[25] For the two SiO_2-like capping layers (films *A* and *B*), Fig. 3(a) shows that up to 29 meV blue shift can be attributed to the sputtering process. For most samples, however, these shifts are insignificant with respect to the measurement uncertainty. Figure 3(b) shows the DC bias voltages that were recorded from the SiO_2 and Si_3N_4 guns during the five depositions. These voltages are related to the energy of the sputtered material, and depend on the applied RF power, Ar pressure, gun geometry and target material. It is clear that the two films deposited with a SiO_2 bias voltage above 200 V correspond to the only samples with any damage-induced PL shifts. During the other three depositions, both sputtering guns recorded lower bias voltages and negligible shifts were observed. On the other hand, half of the PL samples capped with films *A* and *B* also failed to exhibit any marked contribution from the sputtering process.

Figure 4 shows the energy shifts extracted from the SiO_xN_y capped sample areas with respect to the etched areas. In this case, the differential energy shifts are clear, suggesting that IFVD contributed to intermixing with many of the fifteen samples. In some samples, however, negative ΔE_{IFVD} values were observed where the PL peaked at a longer

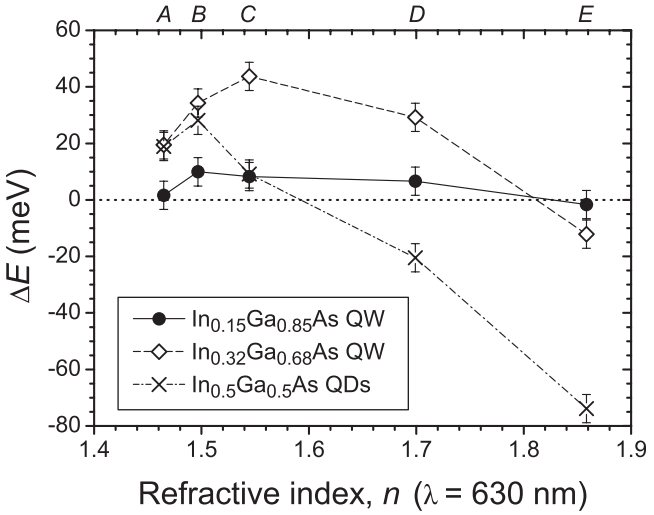

FIG. 4. Energy shifts in the 77 K PL spectra that are ascribed to each SiO_xN_y capping layer present during annealing. Blue shifts ($\Delta E > 0$) indicate impurity-free vacancy disordering whereas negative values indicate suppressed intermixing. The lines between points are included as guides to the eye.

wavelength in the capped area than in the etched area. Whereas a negligible blue-shift in Fig. 4 might indicate minimal IFVD, $\Delta E_{IFVD} < 0$ actually suggests that the capping layer has suppressed the amount of intermixing.

For all three InGaAs structures, positive energy shifts were observed with the oxygen-rich (low index) capping layers and ΔE_{IFVD} peaks for $n \approx 1.5$. For the films with higher refractive indices, the differential energy shifts all decrease and it appears that film *E* suppressed the intermixing in both QW and the QD structures. In general, the ΔE_{IFVD} values extracted for the QW with 15% In are modest, yet the same trend is apparent as in the other structures. Similar shifts were observed for the 32% In QW and the QD samples capped with films *A* and *B*. As the index of the SiO_xN_y film is increased, however, ΔE_{IFVD} falls off rapidly in the QD samples and a large suppression ($\Delta E_{IFVD} = -74$ meV) was observed with film *E*. The $In_{0.32}Ga_{0.68}As$ QW exhibits the highest value of $\Delta E_{IFVD} = 44$ meV with film *C* and a suppression of only 12 meV under film *E*.

B. High-temperature stress

In order to calculate biaxial stress (σ) from the optical profiler measurements, a modified Stoney equation was used. The modification includes the initial radius of curvature (r_0), such that

$$\sigma = \frac{E_s}{1-\nu_s}\frac{t_s^2}{6t_f}(r^{-1} - r_0^{-1}). \quad (1)$$

In this expression, the Young's modulus (E_s) and Poisson's ratio (ν_s) of the substrate are combined as a prefactor, which is the biaxial modulus. For (100) GaAs, $E_s = 85.3$ GPa and $\nu_s = 0.312$.[31] The SiO_xN_y film thicknesses (t_f) were taken from stylus profiler measurements and the substrate thicknesses (t_s) were measured with a Mitutoyo digital gauge. On average, the five GaAs substrates were 364 μm thick and the as-deposited stress in each sputtered film ranged from -0.62 GPa to -0.22 GPa. The negative values indicate compressive stress in all SiO_xN_y films, with the most stress occurring in the highest-index material (film *E*). Although these thick samples exhibited small curvatures, the amount of stress was similar to the values measured from thin GaAs samples.[25]

Given that intermixing occurs at high temperatures, the stress that develops at these temperatures is of primary concern. If the thin capping layer and much thicker substrate are modelled as elastic materials, the rate-of-change in the stress with changing temperature is given by[32]

$$\frac{d\sigma}{dT} = \frac{E_f}{1-\nu_f}(\alpha_s - \alpha_f). \quad (2)$$

In this equation, *T* is the temperature and the biaxial modulus of the film is now significant. So the Young's modulus (E_f) and Poisson's ratio (ν_f) of the film are included in Eq. (2), and the CTE of the film and the substrate are given by α_f and α_s, respectively. The biaxial modulus and CTE of these five SiO_xN_y films have been previously measured, and both properties were found to increase monotonically with refractive index.[25]

The QW and QD samples prepared for PL were annealed at 850 °C and 800 °C, respectively. In order to model the change in stress that develops while heating from 300 K to 1100 K, the CTE of GaAs can be assumed to be constant at the 700 K value[33] of $\alpha_s = 6.74 \times 10^{-6}$ K^{-1}. The thermal stress predicted from Eq. (2) is shown by the solid circles (behind the open squares) in Fig. 5. In this case, the films become more tensile during heating because $\alpha_f < \alpha_s$ for all oxynitride compositions. The thermal stress generally increases with film refractive index, however this trend is not straight-forward. The film CTE values increase with *n*, resulting in a decreasing $\Delta\alpha$ in Eq. (2). On the other hand, the biaxial modulus also increases with refractive index and this is evidently more significant to the predicted thermal stress.

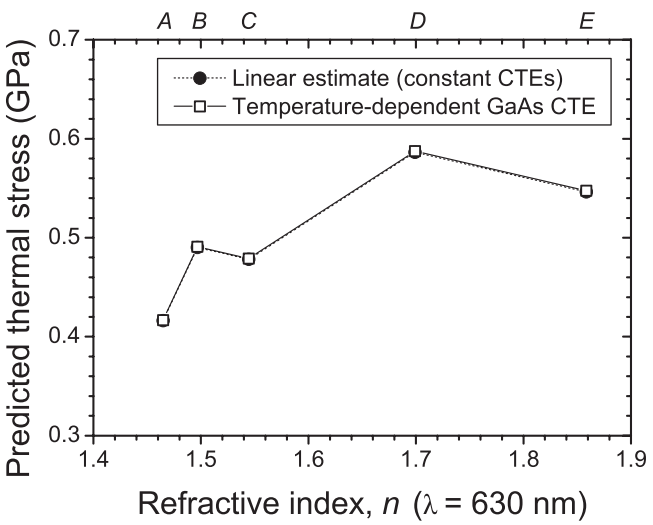

FIG. 5. Thermal stress (from 300 K to 1100 K) predicted from the film properties measured in Ref. 25. The solid circles assume constant thermal expansion in GaAs and the open squares (in front) account for temperature-dependent expansion in GaAs. The thermal expansion in each SiO_xN_y thin film was assumed to be constant in all calculations and the labels along the top axis correspond to these films.

This is a simplified model where the film and substrate CTEs are assumed to be constant with temperature. In fact, the dependence of the GaAs CTE with temperature is well known,[33] and can be summarized as $\alpha_{GaAs} = (0.0016T + 5.63) \times 10^{-6}$ K^{-1}. This linear representation is accurate for 300 K $\leq T \leq$ 1100 K; the Pearson correlation coefficient is 0.998. To calculate the open squares in Fig. 5, this temperature-dependent model was used as α_s and Eq. (2) was integrated over the same temperature range. This method is only a slight improvement in modelling the thermal stress and Fig. 5 shows negligible difference between the two data sets.

The constant SiO_xN_y CTE values were measured at lower temperatures (below 400 °C) and may not be accurate for the high RTA temperatures used in these intermixing experiments. In fact, even if temperature-dependent α_f values up to 1100 K were available for these specific films, they may not actually increase the accuracy of the predicted stress. Deposited films often undergo non-elastic changes when they are first annealed, whereas thermomechanical film properties are typically measured during cooling cycles after such changes have occurred.[25,32] Given that these SiO_xN_y films were deposited near room temperature, structural and compositional changes (for example bond rearrangement and film densification) may be significant for RTA near 1100 K. To illustrate this, five Si samples coated with these oxynitride films were annealed for 60 s at 850 °C. The film thicknesses decreased by an average of 1.5%, as determined by spectroscopic ellipsometry. Such densification produces non-elastic tensile stress in each film. The thermal stress modeled by Eq. (2) does not account for this additional stress.

Although using experimental CTE and biaxial modulus values for each film is more accurate than interpolating bulk SiO_2 and Si_3N_4 values, it is still difficult to model the dielectric-semiconductor system at high temperatures. In order to gain further insight into the effect of stress on IFVD, the high temperature stress was directly measured with the NT9100 optical profiler, as detailed in Sec. II C. Figure 6 shows the stress for each film during heating and cooling ramps with the filled and open symbols, respectively. All SiO_xN_y films become increasingly tensile with heating. For the highest temperatures, this stress increases super-linearly, which may be caused by densification or non-linearities in $\Delta\alpha$. In general, the stress observed during each cooling cycle follows a similar trend. For films *A*, *B* and *C*, the post-annealing stress is somewhat more compressive than beforehand whereas there is negligible net change in film *E*. Film *D* ($n = 1.70$) developed significant compressive stress during cooling, as shown by the open blue stars in Fig. 6. This change is more pronounced than in any of the other samples, however the cause of this difference is not clear.

For presentation clarity in Fig. 6, the curves for films *A*, *B*, *C* and *D* have been offset vertically and the horizontal broken lines indicate zero stress for each data set. The extent of the initial compressive stress is much larger than the as-deposited stress measured after the SiO_xN_y depositions. This is an artifact from cleaving the samples to fit in the TS1500 microscope stage. Hence, the absolute magnitude of the stress in Fig. 6 is not as relevant as the change in stress that develops during heating. This thermal stress (σ_{th}) is shown for films *A* and *E* by the black and red arrows, respectively. These measurements provide insight into the stress in these dielectric-semiconductor systems during high-temperature intermixing processes.

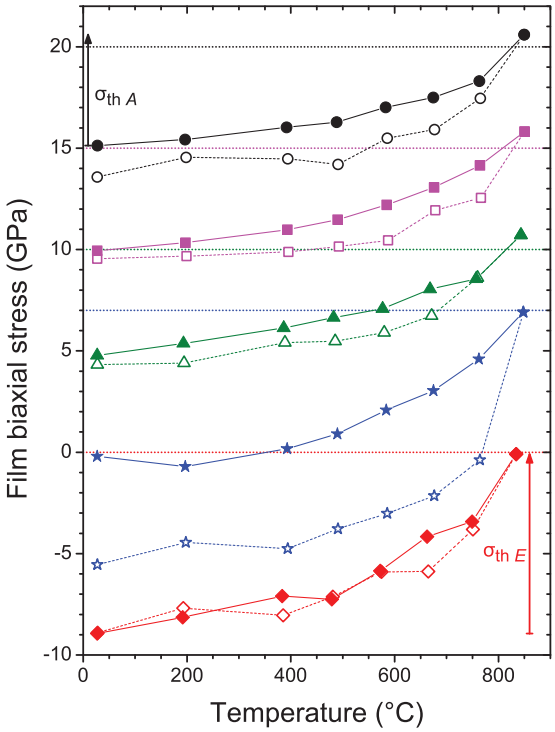

FIG. 6. Measured stress in each SiO_xN_y film during heating to about 1100 K (filled symbols) and then cooling (open symbols). Films *A* (black circles), *B* (magenta squares), *C* (green triangles), *D* (blue stars) and *E* (red diamonds) are labelled in order of increasing refractive index. The horizontal lines indicate nominally zero stress for each set, which have been offset for clarity. The thermal stress (σ_{th}) that developed during heating is indicated for *A* and *E*.

The thick GaAs samples and minimized image-collection times led to some anomalous data points in the otherwise-continuous evolution of film stress in Fig. 6. Nevertheless, the overall σ_{th} values enable the five films to be compared, as shown by the open squares in Fig. 7. Careful scrutiny of

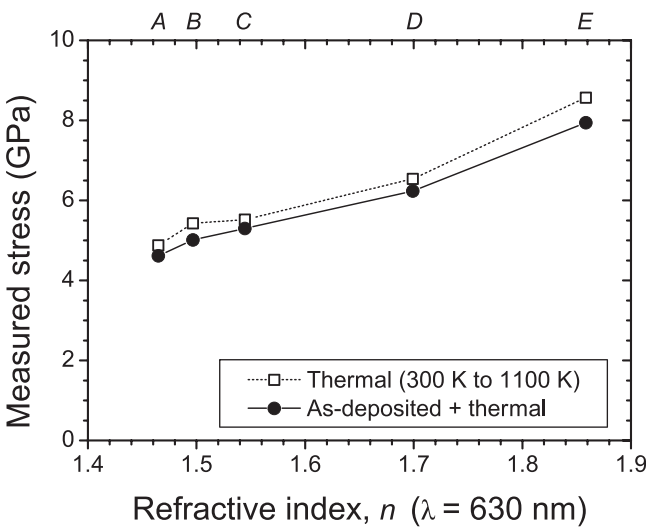

FIG. 7. Biaxial stress measured in each silicon oxynitride thin film. The thermal stress indicates the change in stress when heating from room temperature up to 1100 K (interpolated). The solid circles show the total stress, including the as-deposited measurements.

Fig. 6 will reveal that there are differences in the actual peak temperature (according to the K-type thermocouple) because of a drift in the stage calibration. Therefore, the peak stress values have been interpolated to those at 1100 K to allow comparison of the σ_{th} values.

Clearly the thermal stress in Fig. 7 is more significant for all films than the as-deposited stress that was previously discussed. Furthermore, these measurements are about an order of magnitude higher than the theoretical thermal stress values presented in Fig. 5. This highlights the significance of the non-linearities and non-elastic film changes to this system. Figure 7 shows that despite these differences in magnitude, the thermal component of stress still exhibits similar trends with SiO_xN_y composition. That is, σ_{th} increases monotonically with film refractive index and this behaviour was previously explained by the increasing biaxial modulus. It may also be the case that the nitrogen-rich films are deposited further from structural equilibrium, so they undergo more significant changes during annealing than the oxygen-rich films. The post-annealing tensile stress has also been reported to increase with N content in PECVD SiO_xN_y films, although the presence of H may be a factor in this case.[20] Figure 7 also shows the total film stress, with the filled circular points. This includes the addition of the as-deposited stress but is clearly dominated by the thermal contribution. These results confirm that significant compressive stress is exerted on the GaAs substrate during RTA and that this stress increases with n. In Sec. IV B, these temperature-dependent stress measurements will be related to the degree of intermixing that has been extracted from PL spectroscopy.

IV. DISCUSSION

A. Influence of sputter deposition

Silica films deposited by RF sputtering have been previously shown to promote intermixing at lower temperatures than IFVD with PECVD silica.[23,24] In addition, the magnitudes of the shifts in QW or QD PL spectra can also be larger with sputtered silica. These observations have been transferred to different III-V materials systems, suggesting that the process is separate from the standard IFVD mechanism. Instead, these results have been explained by the creation of point defects on the semiconductor surface during sputter deposition. For example, Kowalski *et al.* removed a sputter-deposited silica cap from their sample and replaced it with PECVD SiO_2 of the same thickness. After subsequent annealing, this sample showed the same PL shifts as samples capped with sputtered silica during annealing.[23] Hence, the initial deposition process was more significant than the encapsulant present during the annealing stage.

During sputter deposition, the DC bias determines the force by which positive ions (such as Ar^+) are attracted to the target and hence the bias is also related to the energy of the sputtered atoms. Material sputtered with a large bias will, on average, reach the substrate with more energy and may result in more surface defects. Presumably, most of this damage to the semiconductor surface occurs at the start of the deposition because the growing film will eventually protect the substrate underneath. High RF powers and the associated large bias voltages will also lead to a more intense, and perhaps a bigger glow-discharge volume. The many high-energy particles in the plasma may also lead to some direct substrate damage, however these effects are minimised in magnetron sputtering (particularly since the gun-to-substrate distance here was relatively large). Instead, neutral adatoms are expected to be predominantly responsible for point defects on the substrate surface. Although these are not directly affected by the DC bias, they may be ejected from the target with high energies if Ar^+ ions are incident under a high bias voltage. As discussed in Sec. III A, a few tens of meV shifts were observed in some samples that correspond to the highest voltages. So it seems plausible that high bias voltages can result in target atoms being liberated with higher energies and indirectly lead to some surface damage.

The PL shifts summarized in Fig. 3(a) have been attributed to the sputtering process itself, however the shifts in most samples were insignificant. As shown in Fig. 3(b), the DC bias voltage observed across the SiO_2 gun was almost 300 V for film *A*, where 300 W RF power was supplied. This intrinsic bias was not directly controlled, however the RF power, process gas, target material and system geometry will affect the observed voltage. This AJA International ATC 2400 -V system uses magnetron sputter deposition, which is designed to confine the plasma away from the substrate holder and minimise such surface damage. On the other hand, Kowalski *et al.* reported a DC bias of 1 kV for only 100 W RF power and it is possible that a different sputtering configuration was employed.[23] In a patent more recently filed by these authors, a diode sputterer is recommended for enhancing QW intermixing.[34] In this case, a pre-etch step in the sputter system was implemented to induce further surface damage. Even so, the subsequent silica deposition by diode sputtering would allow for greater plasma exposure than magnetron sputtering. More surface damage and therefore larger PL shifts would be expected, even without any pre-etching.

B. Influence of SiO_xN_y composition

Rutherford backscattering spectrometry (RBS) and spectroscopic ellipsometry were respectively used to show that the atomic density and refractive index (n) of these silicon oxynitride films increase monotonically from films *A* through to *E*.[25] Increases in n for these SiO_xN_y films may be consistent with a decrease in O content accompanied by an increase in N content and/or the increase in density.[35] The compositions extracted from RBS are in fact consistent with both of these scenarios. In addition, all silicon oxynitride films contained about 1% Ar from the sputtering process.[25] A previous study[27] found that incorporated Ar was desorbed during RTA at 650 °C and it is likely the same is true for the sputtered SiO_xN_y films studied here. The capacity for these oxynitrides to enhance intermixing through IFVD should be predominantly governed by the film density, stoichiometry and biaxial stress during RTA.

The degree of Ga out-diffusion is known to be affected by the film density and composition. Fourier-transform infrared spectroscopy did not indicate the presence of significant

H concentrations in any of these five films.[25] Therefore the degree of Ga out-diffusion would be expected to decrease monotonically with increasing n. Whereas film A is relatively porous and is able to accommodate the soluble Ga atoms, the other oxynitrides are denser and are not so conducive to this out-diffusion. In addition, the high O content in films A and B will promote the metallurgical reactions between the semiconductor and the encapsulant.[35] Therefore the Ga out-diffusion should be enhanced more effectively than in the other films. The PL shifts in Fig. 4, however, do not support this simple explanation. As noted in Sec. III A, the differential energy shifts that should indicate the degree of IFVD do not exhibit a straight-forward trend with respect to film refractive index. Instead, there is an initial increase in ΔE_{IFVD} with n followed by a decrease, such that intermixing was actually suppressed by film E. Although the magnitudes of these shifts differ, this trend is clear in all InGaAs/GaAs structures.

The aforementioned changes in film stoichiometry and density might result in some decrease of ΔE with the higher-index films, however the inhibition of intermixing indicated by $\Delta E < 0$ is not consistent with this explanation. A dense film with $y \gg x$ could be impermeable to Ga and therefore no additional V_{Ga} would be created at the semiconductor surface. In the absence of IFVD, the PL peak energy in the capped sample regions would not be shifted with respect to the HF-etched regions. Instead, the PL observed from the regions capped with SiO_xN_y film E actually peaked at longer wavelengths than the respective etched references.

Suppression of intermixing is often associated with other dielectric capping layers, such as TiO_2. Such films have large thermal expansion coefficients, which result in tensile stress acting on the III-V substrate at high temperatures. Any V_{Ga} that are present in the semiconductor will be trapped at the interface with the dielectric film and hence, they are removed from the vicinity of buried QWs or QDs.[11,14] A different mechanism is responsible in the case of SiO_xN_y film E.

The as-deposited stress was measured in each silicon oxynitride thin film after sputter deposition. The negative values indicated some initial compressive stress in each film (tensile stress in the substrate). The substrates were not heated during sputtering but rather the deposition itself was responsible for this stress. It is well-known that the arrival of energetic adatoms during sputter deposition can transfer momentum to the existing surface material and cause "atomic peening" of the growing film.[36] This can be particularly true with low gas pressures and a reasonably low Ar pressure of 3 mTorr was employed in this work.

Despite these initial film stresses, the SiO_xN_y films studied here have been shown to have CTE values less than GaAs.[25] The CTE mismatch in these samples leads to tensile thermal stress in the five films, as shown by the modelled data in Fig. 5. These values generally increase with film refractive index because the films' biaxial moduli increase with n.[25] In fact, the σ_{th} values that were directly measured while heating the samples to 1100 K are about ten times higher than these predicted values. The sum of the as-deposited and thermal stress components was shown in Fig. 7 for each film. These values increase monotonically with n from 4.6 GPa in film A to 7.9 GPa in film E. In all cases, the films experience tensile stress and therefore compressive stress will be imposed on the III-V material. This is consistent with reports of stress in single layers of similar dielectric thin films.[11,20]

Clearly, a different mechanism must be responsible for the suppressed intermixing under film E than the agglomeration of vacancies that occurs at interfaces with high-CTE capping layers.[11,14] Indeed, it is known that other processes can be related to the extent of intermixing under dielectric capping layers.[13] IFVD using doped silica films has been found to decrease[13] with films that exert higher levels of compressive stress on GaAs-based structures. This can be attributed to the conversion of V_{Ga} to EL2 defects. This conversion, which can be summarized as $V_{Ga} + As_i \rightarrow As_{Ga}$, was shown to be more efficient under compressive stress.[12] On the other hand, it is also known that compressive stress in the semiconductor structure will enhance the mobility of vacancies and can pilot them towards the vicinity of buried quantum structures.[11] Therefore, the actual concentration of V_{Ga} in silica-capped QW or QD structures is the result of competition between the V_{Ga} concentration injected at the III-V surface (plus any as-grown vacancies) that are freely mobile within the lattice, and the concentration of V_{Ga} that are consumed in the creation of As_{Ga} defects.[12] Presumably, a modest amount of compressive stress in the semiconductor is optimal for IFVD as it will allow V_{Ga} movement towards the QWs or QDs (which are usually on the order of 100 nm below the III-V surface), but it will not excessively drive the creation of As_{Ga}.

The fact that ΔE_{IFVD} initially increases with n in Fig. 4 is also consistent with this explanation. It is clear from the SiO_xN_y stoichiometry and density characteristics that film A is the most conducive capping layer for Ga out-diffusion. Figure 7, however, clearly shows small increases in the high-temperature stress in films B and C and this will increase the mobility of the injected vacancies. In fact, films A, B and C all exhibit stoichiometries with $x \gg y$. So the amount of V_{Ga} that are created as $n \rightarrow 1.6$ may not significantly decrease, particularly compared to their increased mobility during RTA.

This explanation is also consistent with a previous QW study, where small amounts of N were added to SiO_x by sputtering in Ar/N_2 mixtures.[27] Up to 11 atomic per cent N was incorporated and this was correlated with an increase in ΔE_{IFVD}. In the higher-index films studied here, however, $x \approx y$ and film E actually contains more N than O. Although Ga out-diffusion will be less in these capping layers, it is the markedly higher stress (above 6 GPa in Fig. 7) that consumes even the as-grown V_{Ga}. Hence, not only does IFVD decrease with these oxynitride films, but thermal intermixing is also inhibited and $\Delta E_{IFVD} < 0$ with film E.

The differences between the three InGaAs/GaAs structures shown in Fig. 4 can be explained by the different group-III concentrations that were discussed in Sec. III A and the lower temperature used to anneal the QD samples. For example, the larger energy shifts observed in the $In_{0.32}Ga_{0.68}As$ QW PL compared to the $In_{0.15}Ga_{0.85}As$ QW PL are due to the larger gradient in In/Ga composition. There is potentially some contribution from the intrinsic strain as well. The QDs

have even higher concentration gradients, large surface areas and high levels of strain.

On the other hand, the QDs were annealed at a lower temperature so these PL shifts for low-index capping layers are in-between the ΔE_{IFVD} values for the two QW structures. With respect to the higher-index films (*D* and *E*), the suppression of intermixing is significantly clearer in the QD PL than with the QW samples. This is most likely related to the difference in annealing temperatures and the competition between the creation and annihilation of V_{Ga}. It is likely that fewer vacancies would have been created at the encapsulant-semiconductor interface during IFVD of the QDs at 800 °C than during the 850 °C anneal of the QW samples. Yet it is possible that rate of V_{Ga} conversion to As_{Ga} is not as sensitive to this temperature difference and a similar amount of vacancies are consumed. Therefore the excess V_{Ga} concentration (compared to the respective as-grown V_{Ga} concentration) under a high-index capping layer is much lower in the QD than the QW structures. Furthermore, there are initially more vacancies present in the as-grown QD material than in the QW structures because of the different MOCVD growth temperatures. Hence, there may also be more V_{Ga} available to be consumed (a larger dynamic range in V_{Ga} concentration) in the QD samples.

V. CONCLUSIONS

In this article, intermixing processes in III-V QWs and QDs have been thoroughly investigated with low-temperature PL spectroscopy. In order to understand the influence of SiO_xN_y capping-layer stoichiometry on the IFVD mechanism, insight into the film structure was necessary. In addition, direct high-temperature stress measurements were performed to further investigate the intermixing process. The tensile film stress at high temperatures was found to be far higher than that predicted from a simple model, even though the thermo-mechanical properties were known for these specific thin films. In addition, this thermal stress was much more significant than the as-deposited compressive film stress that resulted from the sputter deposition process.

The high-temperature solubility of Ga is known to decrease in SiO_xN_y films as their refractive index (and N content) increases. This is particularly true in films that do not contain significant H concentrations, such as these sputtered oxynitrides. With less Ga out-diffusion, fewer vacancies are injected into the III-V matrix and IFVD is less effective. Compared to other capping layers, such as low-temperature PECVD silica, all of these films are relatively dense and so even the low-index SiO_xN_y may not have been optimal for Ga out-diffusion.

It is proposed that the effects of high-temperature stress on vacancy dynamics were actually more influential to the degree of intermixing than the amount of Ga that out-diffused into different capping layers. Although compressive stress was exerted on the GaAs substrates during annealing under all five films, the amount of stress increased with film refractive index. A small increase in this stress may enhance the mobility of V_{Ga} in the III-V lattice such that they can more effectively assist interdiffusion at the QW or QD interfaces. Significantly higher stress, however, may drive the conversion of these vacancies to EL2 (As_{Ga} antisite) defects, therefore rendering the IFVD process inefficient. Moreover, even V_{Ga} that were present in the as-grown samples can be consumed by this mechanism. As a result, intermixing in some samples was actually inhibited by the films with the highest refractive indices. To consolidate this work, a subsequent study might consider a single oxynitride composition of intermediate refractive index (for example with $n \approx 1.6$) and vary the high-temperature stress through another means. For example, depositing a second capping layer of a different dielectric will significantly alter the stress imposed on the III-V substrate during RTA.[11] PL would again be useful to monitor the degree of intermixing in QW or QD layers and a sensitive depth-profiling technique could be used to directly measure the extent of Ga out-diffusion. Deep-level transient spectroscopy could be considered to probe the defects in the III-V matrix under dielectric capping layers. Performing these measurements on epitaxially-grown GaAs samples would avoid the complications that arise from the interfaces in QW or QD structures.[12]

In addition to genuine IFVD, sputter-deposited capping layers have also been linked to a form of intermixing that is universal among several III-V materials systems. This study also considered the potential for these depositions to create point defects in the GaAs surface and therefore initiate this intermixing mechanism. Some modest shifts were recorded that could be attributed to sputter-induced surface damage. These samples all corresponded to depositions with the highest DC bias voltages, however no consistent trend was observed. It was noted that the sputtering configuration employed here and the relatively low DC bias voltages may not be optimal for exploiting this intermixing mechanism. Modifications to the existing sputter system might help to enhance this process. For example, substrates could be placed closer to the magnetron gun, the magnet configuration could be modified or additional bias could be applied to the substrate plate.

There are clearly many factors at play in semiconductor intermixing. IFVD is favored for simplicity, low costs and the ability to tune quantum heterostructures without introducing high levels of impurities. Yet it is often difficult to reproduce the desired degree of intermixing and this is partly due to the plethora of critical experimental parameters. The systematic study presented in this article has examined intermixing with co-sputtered silicon oxynitride capping layers. In particular, the high-temperature stress is of utmost importance to the extent of intermixing and this has been directly measured here. For device applications, large differences in PL energy are desired from selective intermixing and porous SiO_x films are better suited to enhancing intermixing through IFVD. In the case of QDs, however, high levels of thermal intermixing are observed even in the absence of dielectric encapsulants. So it is clear that suppressing the degree of intermixing in certain areas can be a more effective approach to selective intermixing. In terms of the sputtered films studied in this work, silicon oxynitrides with refractive indices of 1.5 and 1.9 can be respectively used to enhance and suppress QD intermixing most effectively.

ACKNOWLEDGMENTS

This work has been made possible with access to the ACT Node of the Australian National Fabrication Facility and through the financial support of the Australian Research Council. The authors are also grateful to Professor Barry Luther-Davies for sharing his expertise with the optical profiler.

[1]E. H. Li, *Semiconductor Quantum Wells Intermixing* (Gordon and Breach, Amsterdam, 2000).
[2]M. Buda, J. Hay, H. H. Tan, L. Fu, C. Jagadish, P. Reece, and M. Gal, "Effects of Zn doping on intermixing in InGaAs/AlGaAs laser diode structures," J. Electrochem. Soc. **150**, G481 (2003).
[3]J. E. Zucker, K. L. Jones, M. A. Newkirk, R. P. Gnall, B. I. Miller, M. G. Young, U. Koren, C. A. Burrus, and B. Tell, "Quantum well interferometric modulator monolithically integrated with 1.55 μm tunable distributed Bragg reflector laser," Electron. Lett. **28**, 1888 (1992).
[4]A. McKee, C. J. McLean, G. Lullo, A. C. Bryce, R. M. De La Rue, J. H. Marsh, and C. C. Button, "Monolithic integration in InGaAs-InGaAsP multiple-quantum-well structures using laser intermixing," IEEE J. Quantum Electron. **33**, 45 (1997).
[5]W. D. Laidig, N. Holonyak, Jr., M. D. Camras, K. Hess, J. J. Coleman, P. D. Dapkus, and J. Bardeen, "Disorder of an AlAs-GaAs superlattice by impurity diffusion," Appl. Phys. Lett. **38**, 776 (1981).
[6]J. H. Marsh, "Quantum well intermixing," Semicond. Sci. Technol. **8**, 1136 (1993).
[7]P. Lever, H. H. Tan, and C. Jagadish, "Impurity free vacancy disordering of InGaAs quantum dots," J. Appl. Phys. **96**, 7544 (2004).
[8]P. N. K. Deenapanray, H. H. Tan, L. Fu, and C. Jagadish, "Influence of low-temperature chemical vapor deposited SiO_2 capping layer porosity on GaAs/AlGaAs quantum well intermixing," Electrochem. Solid-State Lett. **3**, 196 (2000).
[9]P. N. K. Deenapanray and C. Jagadish, "Impurity-free intermixing of GaAs/AlGaAs quantum wells using SiO_x capping: Effect of nitrous oxide flow rate," J. Vac. Sci. Technol. B **19**, 1962 (2001).
[10]S. Bürkner, M. Maier, E. Larkins, W. Rothemund, E. O'Reilly, and J. Ralston, "Process parameter dependence of impurity-free interdiffusion in GaAs/$Al_xGa_{1-x}As$ and $In_yGa_{1-y}As$/GaAs multiple quantum wells," J. Electron. Mater. **24**, 805 (1995).
[11]A. Pépin, C. Vieu, M. Schneider, H. Launois, and Y. Nissim, "Evidence of stress dependence in SiO_2/Si_3N_4 encapsulation-based layer disordering of GaAs/AlGaAs quantum well heterostructures," J. Vac. Sci. Technol. B **15**, 142 (1997).
[12]S. Doshi, P. N. K. Deenapanray, H. H. Tan, and C. Jagadish, "Towards a better understanding of the operative mechanisms underlying impurity-free disordering of GaAs: Effect of stress," J. Vac. Sci. Technol. B **21**, 198 (2003).
[13]P. N. K. Deenapanray, B. Gong, R. N. Lamb, A. Martin, L. Fu, H. H. Tan, and C. Jagadish, "Impurity-free disordering mechanisms in GaAs-based structures using doped spin-on silica layers," Appl. Phys. Lett. **80**, 4351 (2002).
[14]L. Fu, P. Lever, H. H. Tan, C. Jagadish, P. Reece, and M. Gal, "Suppression of interdiffusion in InGaAs/GaAs quantum dots using dielectric layer of titanium dioxide," Appl. Phys. Lett. **82**, 2613 (2003).
[15]M. Osinski, "Monolithic integration of optoelectronic devices using quantum well intermixing," in *State-Of-The-Art Program on Compound Semiconductors XXXVII and Narrow Bandgap Optoelectronic Materials and Devices*, edited by P. Chang, W. Chan, D. Buckley, and A. Baca (Electrochemical Society, Pennington, 2002), Vol. 2002-2014, p. 196.
[16]I. Gontijo, T. Krauss, J. H. Marsh, and R. M. De La Rue, "Postgrowth control of GaAs/AlGaAs quantum well shapes by impurity-free vacancy diffusion," IEEE J. Quantum Electron. **30**, 1189 (1994).
[17]H. S. Lee, A. Rastelli, S. Kiravittaya, P. Atkinson, C. C. B. Bufon, I. Monch, and O. G. Schmidt, "Selective area wavelength tuning of InAs/GaAs quantum dots obtained by TiO_2 and SiO_2 layer patterning," Appl. Phys. Lett. **94**, 161906 (2009).
[18]D. G. Deppe, L. J. Guido, N. Holonyak, Jr., K. C. Hsieh, R. D. Burnham, R. L. Thornton, and T. L. Paoli, "Stripe-geometry quantum well heterostructure $Al_xGa_{1-x}As$-GaAs lasers defined by defect diffusion," Appl. Phys. Lett. **49**, 510 (1986).
[19]W. J. Choi, S. M. Han, S. I. Shah, S. G. Choi, D. H. Woo, S. Lee, S. H. Kim, J. I. Lee, K. N. Kang, and J. Cho, "Dependence of dielectric-cap quantum-well disordering of GaAs-AlGaAs quantum-well structure on the hydrogen content in SiN_x capping layer," IEEE J. Sel. Top. Quantum Electron. **4**, 624 (1998).
[20]J. F. Hazell, D. A. Thompson, N. Bertsch, J. G. Simmons, B. J. Robinson, and G. I. Sproule, "Intermixing of InGaAsP/InGaAsP quantum-well structures using dielectric films," Semicond. Sci. Technol. **16**, 986 (2001).
[21]P. Kordoš, P. Kúdela, D. Gregušová, and D. Donoval, "The effect of passivation on the performance of AlGaN/GaN heterostructure field-effect transistors," Semicond. Sci. Technol. **21**, 1592 (2006).
[22]M. I. Alayo, D. Criado, M. N. P. Carreño, and I. Pereyra, "Fabrication of PECVD-silicon oxynitride-based optical waveguides," Mater. Sci. Eng., B **112**, 154 (2004).
[23]O. P. Kowalski, C. J. Hamilton, S. D. McDougall, J. H. Marsh, A. C. Bryce, R. M. De La Rue, B. Vögele, C. R. Stanley, C. C. Button, and J. S. Roberts, "A universal damage induced technique for quantum well intermixing," Appl. Phys. Lett. **72**, 581 (1998).
[24]D. Bhattacharyya, A. S. Helmy, A. C. Bryce, E. A. Avrutin, and J. H. Marsh, "Selective control of self-organized $In_{0.5}Ga_{0.5}As$/GaAs quantum dot properties: Quantum dot intermixing," J. Appl. Phys. **88**, 4619 (2000).
[25]I. R. McKerracher, L. Fu, H. H. Tan, and C. Jagadish, "Thermal expansion coefficients and composition of sputter-deposited silicon oxynitride thin films," J. Phys. D **43**, 335104 (2010).
[26]L. Fu, P. Lever, K. Sears, H. H. Tan, and C. Jagadish, "$In_{0.5}Ga_{0.5}As$/GaAs quantum dot infrared photodetectors grown by metal-organic chemical vapor deposition," IEEE Electron Device Lett. **26**, 628 (2005).
[27]I. McKerracher, L. Fu, H. Tan, and C. Jagadish, "Impurity-free vacancy disordering of quantum heterostructures with SiOxNy encapsulants deposited by magnetron sputtering," Proc. SPIE **7039**, 70390U (2008).
[28]W. P. Gillin and D. J. Dunstan, "Strain and interdiffusion in semiconductor heterostructures," Phys. Rev. B **50**, 7495 (1994).
[29]S.-W. Ryu, I. Kim, B.-D. Choe, and W. G. Jeong, "The effect of strain on the interdiffusion in InGaAs/GaAs quantum wells," Appl. Phys. Lett. **67**, 1417 (1995).
[30]W. P. Gillin, "Effect of strain on the interdiffusion of InGaAs/GaAs heterostructures," J. Appl. Phys. **85**, 790 (1999).
[31]W. A. Brantley, "Calculated elastic constants for stress problems associated with semiconductor devices," J. Appl. Phys. **44**, 534 (1973).
[32]M. M. de Lima, Jr., R. G. Lacerda, J. Vilcarromero, and F. C. Marques, "Coefficient of thermal expansion and elastic modulus of thin films," J. Appl. Phys. **86**, 4936 (1999).
[33]S. Adachi, "Thermal expansion coefficient of GaAs," in *Properties of Gallium Arsenide*, 3rd ed., edited by M. Brozel and G. Stillman (INSPEC, The Institution of Electrical Engineers, London, 1996), p. 23.
[34]C. J. Hamilton, O. P. Kowalski, J. H. Marsh, and S. D. McDougall, "Method of manufacturing optical devices and related improvements," U.S. patent 6,989,286 (24 January 2006).
[35]P. N. K. Deenapanray, H. H. Tan, M. I. Cohen, K. Gaff, M. Petravic, and C. Jagadish, "Silane flow rate dependence of SiO_x cap layer induced impurity-free intermixing of GaAs/AlGaAs quantum wells," J. Electrochem. Soc. **147**, 1950 (2000).
[36]D. W. Hoffman and J. A. Thornton, "Internal stresses in sputtered chromium," Thin Solid Films **40**, 355 (1977).